



## A Digital Discrete-Time Non-Foster Approach to Broadband Fast-Wave Microstrip Lines

**Thomas P. Weldon and Ryan S. Adams**

University of North Carolina at Charlotte, Dept. of Electrical and Computer Eng., 9201 Univ. City Blvd.,  
Charlotte, NC, 28223, USA  
tpweldon@uncc.edu

**Abstract** – The design of a fast-wave microstrip line is presented, where analog negative capacitance circuits are replaced by digital discrete-time non-Foster circuits. Building upon recent results for a wideband three-section fast-wave microstrip line using three negative capacitors, the proposed digital approach is shown to exhibit fast-wave characteristics over wide bandwidth with phase velocity greater than the speed of light in vacuum. Quality factor of negative capacitors is known to limit bandwidth of analog non-Foster fast-wave lines, and similar behavior is observed in the digital non-Foster simulations. Nevertheless, the proposed digital non-Foster approach is shown to offer broadband fast-wave performance, even with limited quality factor.

### I. INTRODUCTION

Digital discrete-time implementations have been proposed for a number of non-Foster circuit elements such as negative capacitors and negative inductors [1–3]. This digital approach offers an alternative to analog approaches such as Linvill circuits and current-conveyor-based circuits, and may offer advantages in certain applications. [4–6]. Therefore, the following considers the design of a fast-wave transmission line using digital non-Foster circuits [7].

Fast-wave transmission lines are useful in a range of applications including leaky-wave antennas, but conventional metamaterial-based designs often suffer from dispersion and bandwidth limitations [7, 8]. Non-Foster circuits can address bandwidth limitations in fast-wave lines and metamaterials [7, 9–11]. Results in [7] describe a wideband three-section fast-wave microstrip transmission line with non-Foster loading. Therefore, a digital non-Foster fast-wave design is considered below, where the three negative capacitors are replaced by digital discrete-time non-Foster circuits with negative capacitance. The following sections describe the design of digital non-Foster circuits, the fast-wave line, and simulation results for negative capacitance with limited  $Q$  (quality factor).

### II. DIGITAL DISCRETE-TIME NON-FOSTER CIRCUIT AND NON-FOSTER FAST-WAVE MICROSTRIP LINE

As noted above, the three-section fast-wave transmission line being considered requires three negative capacitors of equal value [7]. To implement these negative capacitors, consider the digital discrete-time non-Foster approach shown in Fig. 1(a). The ADC (analog-to-digital converter) with clock period  $T$  generates discrete-time signal  $v_{in}[n] = v_{in}(nT)$  from the continuous-time input voltage  $v_{in}(t)$ . The DAC (digital-to-analog converter) with clock period  $T$  generates continuous time input current  $i_{in}(t)$  from discrete-time signal  $i_{in}[n] = v_{in}[n] * h[n]$ , where  $H(z)$  is the  $z$ -transform of  $h[n]$ , and  $I_{in}(z) = V_{in}(z) H(z)$ . Assuming a DAC with ZOH (zero-order hold), the input impedance is  $Z_{in}(s) = V(s)/I(s) \approx V^*(s)/I(s) = sT/[(1 - z^{-1})H(z)]|_{z=e^{sT}}$  for frequencies below  $0.5/T$  Hz, and where  $V^*(s) = \sum v(nT)e^{-nsT}$  for integer  $n$  is the starred transform [1, 12].

A simple digital negative capacitor can be implemented by approximating continuous-time relation  $i_{in}(t) = C dv_{in}(t)/dt$  by the discrete-time relation  $i_{in}[n] = C(v_{in}[n] - v_{in}[n-1])/T$  and taking the  $z$ -transform,  $I_{in}(z) = C(1 - z^{-1})V_{in}(z)/T$ . Since  $I_{in}(z) = V_{in}(z) H(z)$ , then  $H(z)$  becomes

$$H(z) = C(1 - z^{-1})/T, \quad (1)$$

where  $T$  is the ADC and DAC clock period, and  $C$  is the desired capacitance (positive or negative) [1, 3].

A block diagram of a discrete-time negative capacitor with  $C = -9.5$  pF is shown in Fig. 1(b). To accommodate Keysight ADS large-signal S-parameter simulations, analog samplers and delay lines are used to simulate the

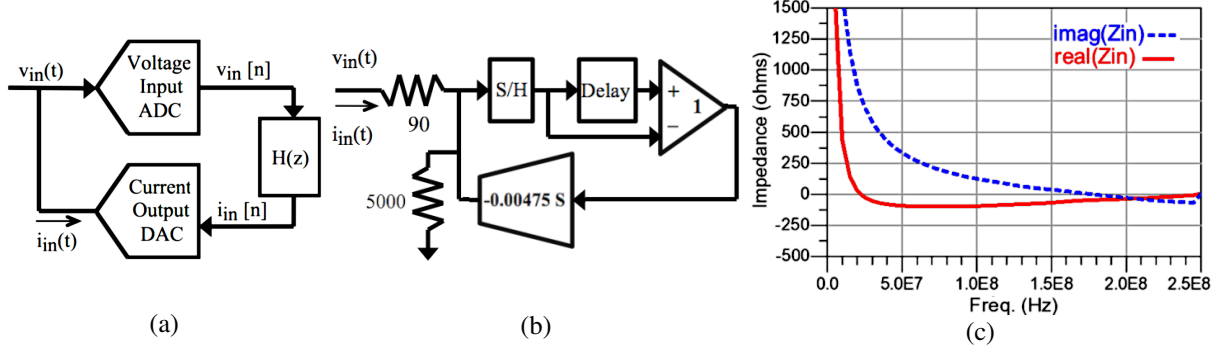


Fig. 1: (a) Block diagram of a digital discrete-time non-Foster circuit [1–3]. Input voltage  $v_{in}(t)$  is converted by the ADC to  $v_{in}[n]$ , processed through z-transform  $H(z)$ , where  $I_{in}(z) = V_{in}(z) H(z)$ , to establish port current  $i_{in}[n]$  to drive the DAC, where the ADC and DAC have high impedance. (b) Block diagram of a discrete-time negative capacitor with  $C = -9.5$  pF. The sample-and-hold (S/H) of clock period  $T = 2$  ns implements the ADC, delay line is 2 ns, and the OTA (operational transconductance amplifier) of  $-0.00475$  S implements the DAC output current. (c) Input impedance  $Z_{in}$  for the example of Fig. 1(b), with the real part of  $Z_{in}$  shown in solid red, the imaginary part of  $Z_{in}$  in dashed blue, and  $Z_{in} = -91 + j334 \Omega$  at 50 MHz, or  $-9.54$  pF in series with  $-91 \Omega$ .

discrete-time signal processing as in [1]. The 90  $\Omega$  and 5000  $\Omega$  resistors are added to adjust Q and stability. Without the two resistors, the overall response of the circuit of Fig. 1(b) is  $i_{in}[n] = -0.00475 (v_{in}[n-1] - v_{in}[n])$ . Comparison with (1) shows  $C/T = -0.00475$ , and thus  $C = -9.5$  pF. Simulation results for the circuit of Fig. 1(b) are shown in Fig. 1(c), confirming a negative capacitance of  $C = -9.54$  pF at 50 MHz with a parasitic series resistance of  $-91 \Omega$ . Stability analyses and methods to reduce parasitic resistance are given in [3] and [1].

### III. SIMULATION RESULTS

To demonstrate the proposed digital non-Foster approach in a fast-wave application, the three-section non-Foster fast-wave microstrip line of Fig. 2(a) was chosen. This example is based on the analog design of Long, Jacob, and Sievenpiper, and provides a baseline for comparison with the proposed digital non-Foster approach [7]. In Fig. 2(a), each of the three line sections in the dashed boxes is comprised of a pair of FR-4 microstrip lines denoted “Tx Line,” with a non-Foster negative capacitance of  $C = -9.5$  pF connected between the pair. In [7], each negative capacitance was previously implemented using an analog circuit. The proposed approach replaces each of the negative capacitors in Fig. 2(a) with the digital non-Foster circuit of Fig. 1(b).

The fast-wave microstrip line was simulated using the digital non-Foster implementation of Fig. 1(b) for the three negative capacitors of Fig. 2(a). Time domain transient simulations were first conducted to verify the circuit was not oscillating or latching [3]. Keysight ADS large-signal S-parameter simulation was then used to measure the S-parameters of Fig. 2(a), with the phase of  $S_{21}$  in degrees given in Fig. 2(b), and with the magnitude of  $S_{21}$  and  $S_{11}$  in dB given in Fig. 2(c) upper plot.

In Fig. 2(b), the phase of  $S_{21}$  in degrees is plotted in solid red for Fig. 2(a). The phase of a plane wave passing through 96 mm in vacuum is plotted in dashed blue as a reference line, or “light line,” as for the 100 mm line in [7]. The long-dashed green curve in Fig. 2(b) is the phase of an “ideal” version of the fast-wave microstrip of Fig. 2(a), where all three capacitors are replaced by ideal  $C = -9.5$  pF capacitors in an ADS S-parameter simulation. The phase of  $S_{21}$  in Fig. 2(b) clearly exhibits the desired fast-wave characteristic, since the phase of  $S_{21}$  (solid red) remains less negative than the phase in vacuum (dashed blue), up to approximately 115 MHz. In addition, the phase of  $S_{21}$  (solid red) closely tracks the “ideal” phase (long-dashed green), up to approximately 75 MHz. (The anomalous behavior at 250 MHz in the plots corresponds to the frequency where Nyquist sampling is violated.) In the upper plot of Fig. 2(c), the magnitude of  $S_{21}$  in dB is in solid red and the magnitude of  $S_{11}$  in dB is in dashed blue. The peak of  $S_{21}$  is approximately 8.6 dB at 140 MHz, with corresponding  $S_{11}$  at 6.0 dB. Similarly, peaks of  $S_{21}$  and  $S_{11}$  greater than 0 dB were observed near 200 MHz in [7], due to gain associated with the parasitic negative resistance of the non-Foster devices.

In [7], it was also noted that the phase velocity of the fast-wave line greatly decreases when the Q of the negative capacitors falls below  $Q = 2$ . The  $Q = |\text{Im}(Z_{in})/\text{Re}(Z_{in})|$  of the digital non-Foster circuit of Fig. 1(b)

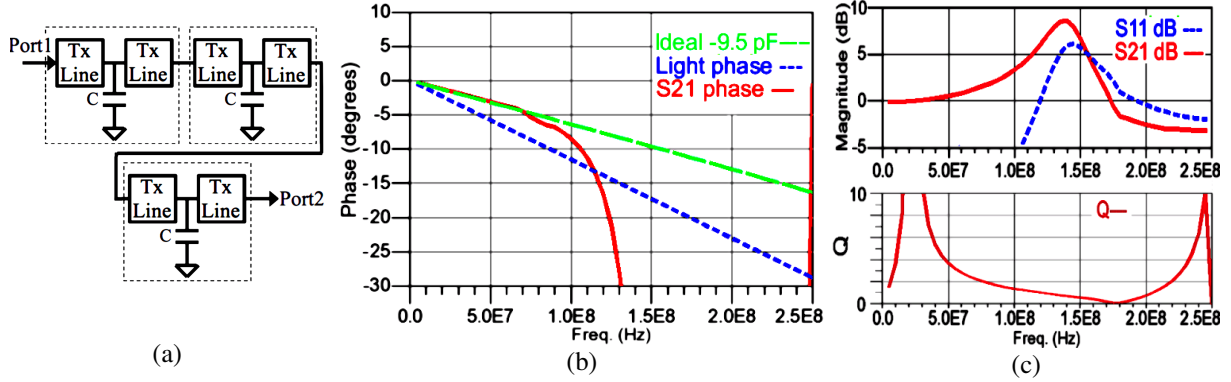


Fig. 2: (a) Block diagram of fast-wave microstrip transmission line comprised of three line sections in dashed boxes, along the lines of [7]. Each of the six “Tx Line” microstrip lines is 16 mm long and 10 mm wide on a 1.57 mm thick FR-4 substrate ( $\epsilon_r = 4.4$ ), and the three  $C = -9.5$  pF loads are Fig. 1(b) digital non-Foster circuits. (b) Phase response. Solid red line is the phase of  $S_{21}$  in degrees for Fig. 2(a), dashed blue “light line” is phase through 96 mm vacuum, long-dashed green line is an “ideal” phase reference, using ideal  $C = -9.5$  pF capacitors. (c) Upper plot is magnitude in dB of  $S_{21}$  (solid red) and  $S_{11}$  (dashed blue) for Fig. 2(a). Lower plot is simulated  $Q = |\text{Im}(Z_{in})|/\text{Re}(Z_{in})$  for the the  $C = -9.5$  pF discrete-time negative capacitor of Fig. 1(b).

and Fig. 1(c) is plotted in Fig. 2(c) lower plot. In this,  $Q > 2$  from 5 MHz to 75 MHz, and falls below unity at 115 MHz. It is observed that fast-wave behavior in the present design ceases near 115 MHz, where the phase of  $S_{21}$  (solid red line in Fig. 2(b)) first becomes more negative than the phase in vacuum (dashed blue line in Fig. 2(b)).

#### IV. CONCLUSION

A fast-wave microstrip line has been designed using digital discrete-time non-Foster circuits to implement negative capacitance. Simulation results show broadband fast-wave performance, where bandwidth appears to be limited by finite  $Q$  of the digital negative capacitors, as noted in [7]. The digital negative capacitors had  $Q > 2$  from 5 MHz to 75 MHz.

#### ACKNOWLEDGMENT

This material is based upon work supported by the National Science Foundation under Grant No. ECCS-1101939.

#### REFERENCES

- [1] T. Weldon, J. Covington, K. Smith, and R. Adams, “Performance of digital discrete-time implementations of non-Foster circuit elements,” in *2015 IEEE Int. Symp. on Circuits and Systems (ISCAS)*, in press, May 2015, pp. 1–4.
- [2] T. P. Weldon, “Digital discrete-time non-Foster circuits and elements,” International Patent Application No. PCT/US2015/27789, Apr. 27, 2015.
- [3] T. Weldon, J. Covington, K. Smith, and R. Adams, “Stability conditions for a digital discrete-time non-Foster circuit element,” in *IEEE Antennas and Propagation Society International Symposium (APSURSI)*, Jul. 2015, in press.
- [4] A. Sedra and K. Smith, “A second-generation current conveyor and its applications,” *IEEE Trans. Circuit Theory*, vol. 17, no. 1, pp. 132–134, 1970.
- [5] J. Linvill, “Transistor negative-impedance converters,” *Proc. of the IRE*, vol. 41, no. 6, pp. 725–729, Jun. 1953.
- [6] S. Stearns, “Incorrect stability criteria for non-Foster circuits,” in *IEEE Antennas and Propagation Society International Symposium (APSURSI)*, Jul. 2012, pp. 1–2.
- [7] J. Long, M. Jacob, and D. Sievenpiper, “Broadband fast-wave propagation in a non-Foster circuit loaded waveguide,” *IEEE Trans. Microw. Theory Tech.*, vol. 62, no. 4, pp. 789–798, Apr. 2014.
- [8] W. Menzel, “Planar leaky-wave antennas - early concepts and actual results,” in *Microwave Conference (EuMC), 2013 European*, Oct. 2013, pp. 483–486.
- [9] P.-Y. Chen, C. Argyropoulos, and A. Alù, “Broadening the cloaking bandwidth with non-Foster metasurfaces,” *Phys. Rev. Lett.*, vol. 111, p. 233001, Dec. 2013.
- [10] S. Saadat, M. Adnan, H. Mosallaei, and E. Afshari, “Composite metamaterial and metasurface integrated with non-Foster active circuit elements: A bandwidth-enhancement investigation,” *IEEE Trans. Anten. Prop.*, pp. 1210–1218, Mar. 2013.
- [11] S. Hrabar, I. Krois, I. Bonic, and A. Kirichenko, “Ultra-broadband simultaneous superluminal phase and group velocities in non-Foster epsilon-near-zero metamaterial,” *Applied Physics Letters*, vol. 102, no. 5, pp. 054 108–1–5, 2013.
- [12] C. Phillips and H. Nagle, *Digital Control System Analysis and Design*. Prentice-Hall, 1990.